Neuropathology and Applied Neurobiology (2016), **42**, 639–653 doi: 10.1111/nan.12288

The identification of raft-derived tau-associated vesicles that are incorporated into immature tangles and paired helical filaments

T. Nishikawa*, T. Takahashi*, M. Nakamori*, N. Hosomi*, H. Maruyama*, Y. Miyazaki†, Y. Izumi† and M. Matsumoto*

**Department of Clinical Neuroscience and Therapeutics, Hiroshima University Graduate School of Biomedical and Health Sciences, Hiroshima and †Department of Clinical Neuroscience, Institute of Health Biosciences, Graduate School of Medicine, University of Tokushima, Tokushima, Japan*

T. Nishikawa, T. Takahashi, M. Nakamori, N. Hosomi, H. Maruyama, Y. Miyazaki, Y. Izumi, M. Matsumoto (2016) *Neuropathology and Applied Neurobiology* **42**, 639–653
The identification of raft-derived tau-associated vesicles that are incorporated into immature tangles and paired helical filaments

Aims: Neurofibrillary tangles (NFTs), a cardinal pathological feature of neurodegenerative disorders, such as Alzheimer's disease (AD) are primarily composed of hyper-phosphorylated tau protein. Recently, several other molecules, including flotillin-1, phosphatidylinositol-4,5-bisphosphate [PtdIns(4,5)P2] and cyclin-dependent kinase 5 (CDK5), have also been revealed as constituents of NFTs. Flotillin-1 and PtdIns(4,5)P2 are considered markers of raft microdomains, whereas CDK5 is a tau kinase. Therefore, we hypothesized that NFTs have a relationship with raft domains and the tau phosphorylation that occurs within NFTs. **Methods**: We investigated six cases of AD, six cases of other neurodegenerative diseases with NFTs and three control cases. We analysed the PtdIns(4,5)P2-immunopositive material in detail, using super-resolution microscopy and electron microscopy to elucidate its pattern of expression. We also investigated the spatial relationship between the PtdIns(4,5)P2-immunopositive material and tau kinases through double immunofluorescence analysis. **Results**: Pretangles contained either paired helical filaments (PHFs) or PtdIns(4,5)P2-immunopositive small vesicles (approximately 1 μm in diameter) with nearly identical topology to granulovacuolar degeneration (GVD) bodies. Various combinations of these vesicles and GVD bodies, the latter of which are pathological hallmarks observed within the neurons of AD patients, were found concurrently in neurons. These vesicles and GVD bodies were both immunopositive not only for PtdIns(4,5)P2, but also for several tau kinases such as glycogen synthase kinase-3β and spleen tyrosine kinase. **Conclusions**: These observations suggest that clusters of raft-derived vesicles that resemble GVD bodies are substructures of pretangles other than PHFs. These tau kinase-bearing vesicles are likely involved in the modification of tau protein and in NFT formation.

Keywords: Alzheimer's disease, granulovacuolar degeneration, lipid raft, pretangle, signaling endosome, tau

Introduction

Alzheimer's disease (AD) is pathologically characterized by the pathological presence of extracellular neuritic plaques, polymorphous amyloid beta protein deposits, and intracellular neurofibrillary tangles (NFTs) composed of

Correspondence: Tetsuya Takahashi, 1-2-3 Kasumi, Minami-ku, Hiroshima 734-8551, Japan. Tel: +81 82 257 5201; Fax: +81 82 505 0490; E-mail: tetakaha@hiroshima-u.ac.jp

Table 1. Subject characteristics

Case no.	*Diagnosis*	*Gender*	*Age*	*GVD stage*	*Aβ* phase	*NFT stage*	*CERAD*	*AD neuro-pathologic change*
1	AD	M	73	5	5	6	Frequent	High
2	AD	F	66	5	5	6	Frequent	High
3	AD	F	75	5	5	6	Frequent	High
4	AD	F	85	5	5	5	Frequent	High
5	AD	F	72	5	5	5	Frequent	High
6	AD	M	88	5	5	5	Frequent	High
7	MyD	M	57	4	3	2	Sparse	Low
8	PKAN	F	57	5	1	5	Sparse	Low
9	CBD	F	75	2	3	3	Frequent	Intermediate
10	PD	M	86	1	4	2	Frequent	Low
11	MSA	F	72	1	3	2	Frequent	Low
12	ALS	F	67	1	3	1	Sparse	Low

AD, Alzheimer's disease; MyD, myotonic dystrophy; PKAN, pantothenate kinase-associated neurodegeneration; CBD, corticobasal degeneration; PD, Parkinson's disease; MSA, multiple system atrophy; ALS, amyotrophic lateral sclerosis; F, female; M, male; Age, age at death; GVD, granulovacuolar degeneration; NFT, neurofibrillary tangle; CERAD, the Consortium to Establish a Registry for Alzheimer's Disease.

hyper-phosphorylated tau. Granulovacuolar degeneration (GVD) bodies are also pathological hallmarks in the neurons of AD patients [1]. We previously reported that charged multivesicular body protein 2B (CHMP2B), an endosome-related protein, and cyclin-dependent kinase 5 (CDK5), a tau kinase, are present in GVD bodies [2,3]. We have also revealed that phosphatidylinositol-4,5-bisphosphate [PtdIns(4,5)P2], a phospholipid associated with lipid rafts, exhibits identical immunoreactivity in GVD bodies and NFTs [4]. In addition, double immunofluorescence staining revealed that PtdIns(4,5)P2-immunopositive granules within NFTs were not colocalized with phosphorylated tau. These results led us to speculate that GVD bodies and NFTs share components in terms of their origin but have different modes of formation.

Paired helical filaments (PHFs) formed by hyperphosphorylated tau protein are the major components of NFTs; however, several molecules in addition to the tau protein, such as flotillin-1 [5], glycogen synthase kinase (GSK)-3β [6], casein kinase 1 (CK-1) [7–9] and CDK5 [10,11], have been detected in NFTs. The pathological consequences of the presence of these molecules have not yet been fully shown. In addition, through electron microscopic observations, Okamoto *et al.* [12] reported the accumulation of small vesicles and GVD bodies adjacent to PHFs. These results suggest that some uncharacterized materials other than PHFs might be novel components of NFTs.

In the present study, we aimed to explore these non-PHF materials in NFTs using super-resolution microscopy and electron microscopy and to address the potential pathological consequences of their presence.

Materials and methods

Subjects

Six cases of AD [mean age = 76.5 years ± 8.4 standard deviations of the mean (SDM)] and six cases of other neurodegenerative diseases with NFTs [mean age = 69.0 years ± 11.2 SDM], including one case each of myotonic dystrophy, pantothenate kinase-associated neurodegeneration (PKAN), corticobasal degeneration, Parkinson's disease (PD), multiple system atrophy (MSA) and amyotrophic lateral sclerosis, were selected. Three control cases [67-year-old female, 70-year-old female, 73-year-old female] free of tau pathology (Aβ phase = 0, NFT stage = 0) were also examined. The clinical profiles, GVD stages [13], Thal phases of amyloid beta protein deposition [14], Braak NFT stages [15], frequency of neuritic plaques according to the method of the Consortium to Establish a Registry for Alzheimer's Disease [16], and degrees of AD neuropathologic change [17] of these patients are shown in Table 1. The use of human materials conformed to the ethical guidelines of Hiroshima University Graduate School of Biomedical and Health Sciences, Hiroshima, Japan. All AD cases fulfilled the quantitative neuropathological criteria for the diagnosis of AD of the National Institute on Aging-Alzheimer's Association guidelines for the neuropathologic assessment of AD;

that is, an AD Neuropathologic Change score of A3, B3 or C3 [17].

Brain tissue

Autopsies were performed within 24 h of death. Brains were fixed in 10% (v/v) formalin for 3 weeks, and 3-μm- or 5-μm-thick paraffin-embedded sections were prepared for subsequent procedures unless otherwise indicated. Unless otherwise indicated, we observed the subiculum and cornu ammonis (CA) subfields 1–4.

Antibodies

The following antibodies were used for the immunohistochemistry and immunofluorescence studies: mouse monoclonal IgM-type anti-PtdIns(4,5)P2 (2C11, dilution 1:500 for immunohistochemistry, 1:100 for immunofluorescence staining; Santa Cruz Biotech, Santa Cruz, CA, USA); mouse monoclonal IgG-type anti-phosphorylated tau [(AT8, dilution 1:800; Innogenetics, Ghent, Belgium), (AT100, dilution 1:100; Thermo Scientific Pierce, Carlsbad, CA, USA), (AT270, dilution 1:200; Thermo Scientific Pierce; mouse monoclonal)], IgG-type anti-Asp421 truncated tau (Tau-C3, dilution 1:200; Invitrogen, Frederick, MN, USA), anti-tau (3-repeat isoform RD3) (8E6/C11, dilution 1:300; Merck Millipore, Darmstadt, Germany) and anti-tau (4-repeat isoform RD4) (1E1/A6, dilution 1:100; Merck Millipore); and rabbit polyclonal anti-CHMP2B (ab33174, dilution 1:600; Abcam, Cambridge, UK), anti-phosphatidylinositol-binding clathrin assembly protein (PICALM) (HPA019053, dilution 1:200; Sigma-Aldrich, St. Louis, MO, USA), anti-phosphorylated mitogen-activated protein kinase kinase (pMEK) 1/2 (Ser217/221) (dilution 1:50; New England BioLabs, Ipswich, MA, USA), anti-GSK-3β [pY216]/GSK-3α [pY279] (44-604G, dilution 1:100; Life Technologies, Carlsbad, CA, USA), anti-phosphorylated spleen tyrosine kinase (pSyk) (AP3271a, dilution 1:50; Abgent, San Diego, CA, USA) and anti-CK-1δ (ab85320, dilution 1:50; Abcam).

Immunohistochemistry

The sections were deparaffinized and rehydrated. For antigen retrieval, sections were microwaved in distilled water for 10 min, followed by washing in phosphate-buffered saline (PBS) for 3 min. Deparaffinized sections were then incubated with 3% H_2O_2 in PBS for 60 min to eliminate endogenous peroxidase activity in the tissue. Each section was incubated overnight at 4°C with the primary antibodies described above. The sections were then washed three times in PBS and incubated with horseradish peroxidase (HRP)-conjugated anti-mouse or anti-rabbit antibodies for 30 min at room temperature. The avidin–biotin complex method was used to detect the mouse monoclonal IgM-type anti-PtdIns(4,5)P2 (clone 2C11) antibody. The sections were then washed three times in PBS and incubated at room temperature with 3, 3-diaminobenzidine (Dako, Glostrup, Denmark).

Quantitative analysis

Quantitative analysis of PtdIns(4,5)P2-positive neurons was performed for different regions of the hippocampus, including CA1, CA2–4 and the subiculum. The numbers of neurons-containing PtdIns(4,5)P2-positive structures were counted sequentially over the entire area, using light microscopy at 400× magnification. We counted the neurons-containing GVD bodies, NFTs and combined structures separately and evaluated the numbers in different regions.

Immunofluorescence staining

We also performed double staining on sections, including sections from the hippocampus and parahippocampal gyrus, for further characterization. First, paraffin-embedded sections were irradiated with UV light overnight at 4°C to reduce autofluorescence by photobleaching the tissue sections. After irradiation, we applied the same primary antibodies described above. The mouse monoclonal IgM-type anti-PtdIns(4,5)P2 (clone 2C11) antibody was detected using a Fluorescein Avidin DCS kit (A-1100; Vector Laboratories, Burlingame, CA, USA). The other primary antibodies were detected using the tyramide signal amplification (TSA) method with HRP-conjugated secondary antibodies and the TSA™ KIT#4, which contains Alexa Fluor™ 568 tyramide (Invitrogen™, Eugene, OR, USA). In cases using both anti-mouse IgM and anti-mouse IgG antibodies as secondary antibodies, a goat polyclonal HRP-conjugated anti-mouse IgG Fc fragment antibody (ab97265, dilution 1:1000; Abcam) was used to detect

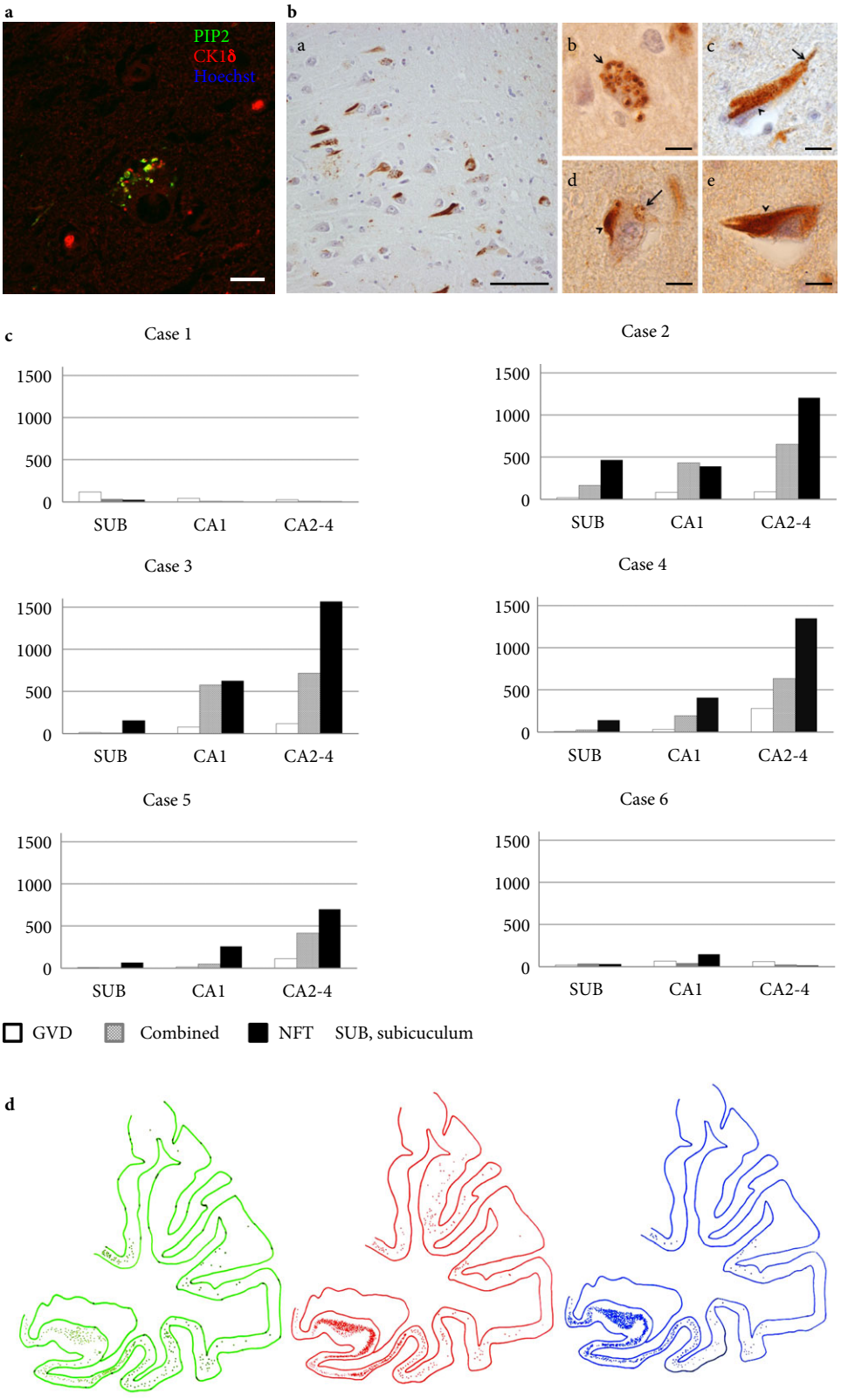

the mouse monoclonal IgG-type primary antibody to prevent cross-reactions between the anti-mouse IgM and IgG antibodies. The slides were mounted with Vectashield (Vector Laboratories) and observed under an LSM 510 confocal laser-scanning microscope (Carl Zeiss AG, Oberkochen, Germany). After obtaining images showing double staining for PtdIns(4,5)P2 and CHMP2B, PtdIns(4,5)P2 and AT8, PtdIns(4,5)P2 and RD3, or PtdIns(4,5)P2 and RD4, the same sections were subjected to Gallyas staining, and the same microscope field was identified [18].

To quantify the degree of colocalization of PtdIns (4,5)P2 with AT8, we performed fluorescence intensity line scanning using ZEN Software (Carl Zeiss AG), and the Pearson product-moment correlation coefficients were obtained, using Microsoft Excel 2007 according to a previously reported method [19].

3D structured illumination microscopy (3D-SIM)

Furthermore, to observe the detailed spatial pattern of PtdIns(4,5)P2 and AT8 by super-resolution imaging with three-dimensional structured illumination microscopy (3D-SIM), 3-μm-thick sections were subjected to double immunofluorescence staining for PtdIns(4,5)P2 and AT8, using the following secondary antibodies: Alexa Fluor™ 488 goat anti-mouse IgM mu chain-specific (ab150121, dilution 1:1000; Abcam) and Alexa Fluor™ 568 goat anti-mouse IgG (dilution 1:1000; Molecular Probes, Eugene, OR, USA). The slides were coverslipped with Vectashield 1000 and cover glass (170 μm in thickness, grade no. 1S) and were observed under a DeltaVision OMX V4 system (GE Healthcare, Washington, DC, USA) equipped with 405, 488, 568, and 642 nm solid lasers, sCMOS cameras (PCO Edge, 2K × 2K, PCO), and a 60×/1.42 NA plan Apochromat oil-immersion objective (Olympus, Tokyo, Japan). The super-resolution images were obtained as previously described [20]. Briefly, optical transfer functions were created for each colour channel from recordings of 0.1-μm-diameter fluorescent beads. 3D-SIM image stacks were reconstructed, using the softWoRx software package, version 6.1.1 (GE Healthcare) with the following settings: pixel size 80 nm; channel-specific optical transfer functions; Wiener filter 0.001; keeping negative intensities; default background intensity value of 65; drift correction with respect to the first angle; and custom K0 guess angles for camera positions.

Electron microscopy

The subiculum of the hippocampus was fixed in 9% formaldehyde, cut into small pieces, postfixed in 1% osmium tetroxide for 2 h, dehydrated and embedded in epoxy resin. Specimens were subjected to electron microscopic analysis. Full-thickness blocks were cut, rapidly placed in cold buffered glutaraldehyde and fixed for 18–20 h at 4°C. The strips were rinsed in PBS and further fixed in osmium tetroxide for 1 h at room temperature; then, they were dehydrated in ethanol and embedded in Epon. One-micrometer sections that were stained with toluidine blue were used for the correlation analysis and for the selection of areas for EM study. Thin sections were cut with a diamond knife, stained with uranyl acetate and lead citrate, and examined under a JEM-1230 (JOEL, Tokyo, Japan) transmission electron microscope.

Results

Various patterns of PtdIns(4,5)P2 immunoreactivity are found in pyramidal neurons of individuals with AD and other neurodegenerative diseases

Some PtdIns(4,5)P2-immunopositive materials exhibited 3- to 5-μm-diameter vesicular structures with

Figure 1. Double immunofluorescence staining for phosphatidylinositol-4,5-bisphosphate [PtdIns(4,5)P2] (green) and casein kinase 1δ (CK-1δ) (red) (**A**). CK-1δ, a marker of granulovacuolar degeneration (GVD) bodies, localized with PtdIns(4,5)P2, suggesting that PtdIns (4,5)P2 is a constituent of GVD bodies. Immunohistochemistry for PtdIns(4,5)P2 in neuronal cells in tissue from several Alzheimer's disease (AD) cases (**B**). Fine PtdIns(4,5)P2-immunopositive granules accumulated in the shape of neurofibrillary tangles. Some of the PtdIns(4,5)P2-immunopositive structures resemble GVD bodies (arrows), and others resemble Neurofibrillary tangles (NFTs) (arrowheads). The neuronal cells that contained PtdIns(4,5)P2-immunopositive structures were classified into three types: those with only GVD body, those with only NFT, and those with both structures. The numbers of neurons containing only GVD body-like structures, only NFT-like structures, and those with both structures in the subiculum, CA1 and CA2–4 of the hippocampus in each AD case (**C**). Schematic representation of the distribution of PtdIns (4,5) P2-positive only GVD body-like structures, only NFT-like structures, and those with both structures in the temporal lobe of an AD patient (case 4) (**D**). Each dot represents a cell containing GVD bodies (green), NFTs (red) or both (blue). Scale bars: (**A**) 10 μm (**B**, a) 100 μm (**B**, b–e) 10 μm.

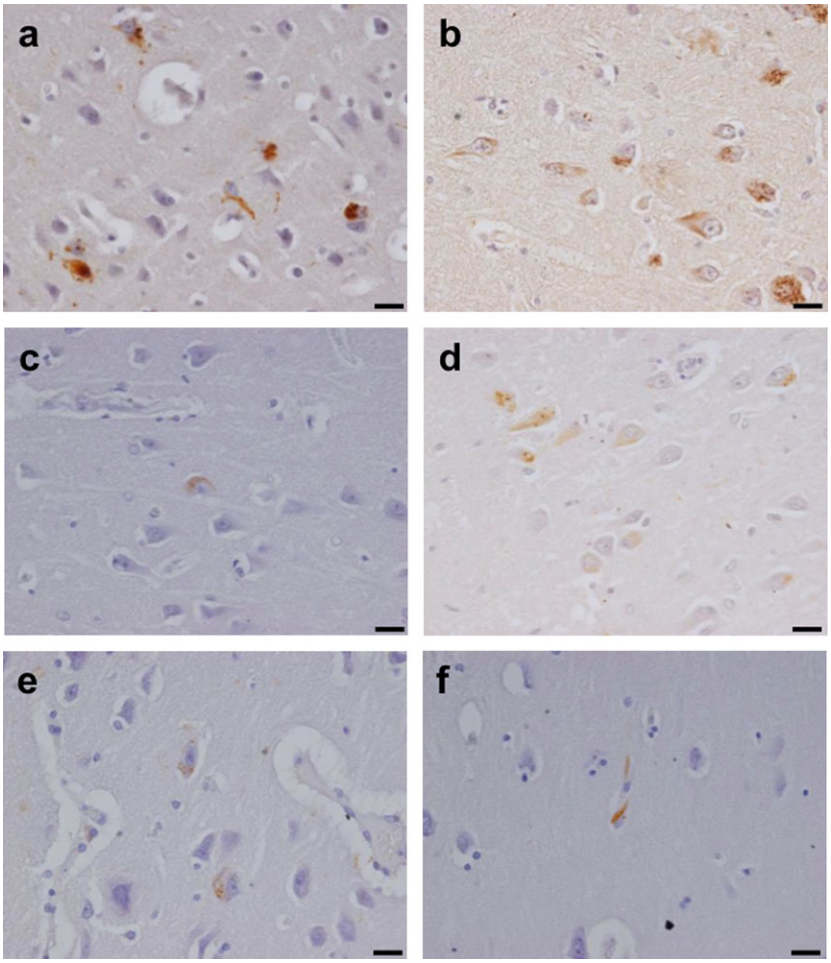

Figure 2. Immunohistochemistry for phosphatidylinositol-4,5-bisphosphate [PtdIns(4,5)P2] in neuronal cells in tissue samples from patients with other neurodegenerative diseases. Neuronal cells containing PtdIns(4,5)P2-immunopositive structures similar to those in the Alzheimer's disease samples were observed in myotonic dystrophy (**a**), pantothenate kinase-associated neurodegeneration (**b**), corticobasal degeneration (**c**), Parkinson's disease (**d**), multiple system atrophy (**e**) and amyotrophic lateral sclerosis (**f**). Scale bars: 20 μm.

central granules that were surrounded by a halo-like clear zone and an outer membrane, characteristics that are indicative of GVD bodies. CK-1δ, a marker of GVD bodies [9,13], was colocalized with PtdIns(4,5)P2, suggesting that PtdIns(4,5)P2 is a constituent of GVD bodies, as previously reported (Figure 1**A**) [4]. The other PtdIns(4,5)P2-immunopositive materials exhibited granules that were clustered and piled up like NFTs. Some neurons contained both types of structures, and others had only one or the other (Figure 1**B**).

The median numbers of neurons containing only PtdIns(4,5)P2-positive GVD bodies in the subiculum, CA1 and CA2–4 of the hippocampus were 15.5, 53.5 and 101 respectively, in the samples from the patients with AD. Those containing PtdIns(4,5)P2-positive NFTs only were 104 (subiculum), 322.5 (CA1), and 947.5 (CA2–4). A considerable number of neurons contained both GVD bodies and NFTs (Figure 1**C**), but only a small number (<15) of each PtdIns(4,5)P2-positive structure was observed in all fields in the samples from the non-tauopathy control. The distribution patterns of each structure were similar throughout the temporal lobe, although they were predominantly located in the hippocampus (Figure 1**D**).

In the samples from individuals with other neurodegenerative diseases, neuronal cells containing smaller PtdIns(4,5)P2-immunopositive granular structures that were shaped like NFTs and/or larger GVD body-like vesicular structures were also observed mainly in the hippocampus; however, many fewer of these cells were observed in the samples from patients with other neurodegenerative diseases than in the AD tissue (Figure 2).

Similar-staining patterns of PtdIns(4,5)P2-immunopositive materials were also observed in the other AD cases.

PtdIns(4,5)P2-immunopositive small granules are present within pretangles and NFTs at a relatively early stage

Double immunofluorescence staining for PtdIns(4,5)P2 and several proteins related to GVD bodies or NFTs revealed the presence of PtdIns(4,5)P2-immunopositive granules, which were smaller than GVD bodies and were surrounded by phosphorylated tau (Figure 3). These PtdIns(4,5)P2-immunopositive granules were immunonegative for CHMP2B (Figure 3**a**). Furthermore, the signal for these PtdIns(4,5)P2-immunopositive granules did not overlap with that for AT8 (Figure 3**c**).

From the viewpoint of tangles, the signal for the PtdIns(4,5)P2-immunopositive granules clearly colocalized with that for RD4 (Figure 3**e**) but only partially colocalized with that for RD3 (Figure 3**g**). In addition, some of these granules were present in the part of the cytoplasm of the neuronal cells that was negative for Gallyas-Braak staining (Figure 3**b**, **d**, **f**, **h**). Hara *et al.* [21] reported that an intraneuronal profile shift from RD3−/4+ pretangles to RD3+/4− ghost tangles by way of RD3+/4+ NFTs might be the basis of the regional gradation that occurs during the progression of NFT pathology. In our study, the PtdIns(4,5)P2-immunopositive granules were immunopositive for RD4 but not for RD3, a characteristic that is similar to that of pretangles. The Tau-C3 antibody specifically recognizes the form of tau that is truncated at Asp421 [22]; this truncation is an early molecular event in tau aggregation that occurs prior to PHF formation [23]. By contrast, mature NFTs exhibit positive AT100 (pT212 and pS214) and AT270 (pT181) immunoreactivity [23,24]. PtdIns(4,5)P2 was not colocalized with AT100 or AT270, but was colocalized with Tau-C3, which also suggests that PtdIns(4,5)P2 is associated with an early stage of NFT development (Figure 3**i**–**l**).

PtdIns(4,5)P2-immunopositive small granules are colocalized with PICALM, pMEK and the tau kinases GSK-3β and pSyk

Phosphatidylinositol-binding clathrin assembly protein is colocalized with phosphorylated tau not only in NFTs but also in GVD bodies [25]. In the present study, double immunofluorescence staining for PtdIns(4,5)P2 and PICALM revealed that PtdIns(4,5)P2-immunopositive fine granules were colocalized with PICALM (Figure 3**m**, **n**) and pMEK (Figure 3**o**, **p**). Furthermore, the signals for several tau kinases, such as GSK-3β and pSyk, which is a newly identified tau kinase [26] that is expressed in hippocampal pyramidal neurons of AD patients and detected in GVD bodies [27], were found to colocalize with PtdIns(4,5)P2-immunopositive fine granules (Figure 3**q**–**t**).

PtdIns(4,5)P2-immunopositive small granules are segregated from phosphorylated tau proteins within NFTs in pyramidal neurons

Although single neurons showed immunoreactivity for both PtdIns(4,5)P2 and AT8, distinct distribution patterns were detected that showed that PtdIns(4,5)P2 and AT8 are mutually exclusive, as previously reported [27] (Figure 4**a**–**c**). A representative fluorescence intensity line scan profile is shown in Figure 4**d**. The peaks for PtdIns(4,5)P2 and AT8 appeared alternately, and the Pearson coefficient for the correlation between the fluorescence intensities was 0.406, indicating a relatively low correlation between the locations of PtdIns (4,5)P2 and AT8.

Super-resolution microscopic images of PtdIns(4,5) P2-immunopositive materials within GVD bodies and NFTs are shown in Figure 4**e**–**h**. Some accumulations of PtdIns(4,5)P2-immunopositive granules were observed in the cytoplasm of a pyramidal cell in the hippocampus of an AD patient, indicative of GVD bodies. On the other hand, scattered PtdIns(4,5)P2-immunopositive small granules were located adjacent to accumulations of AT8-positive granules, indicative of NFTs. As revealed by immunohistochemistry, inside a GVD body, both the granules surrounded by a vesicle, and the vesicle itself were positively stained for PtdIns (4,5)P2; however, based on immunofluorescence staining, within a GVD body, immunoreactivity for PtdIns (4,5)P2 seemed to be present only on granules within a vesicle and not on the outer membrane.

GVD body-like small vesicles are located adjacent to PHFs

An ultrastructural image of a pyramidal cell in the subiculum of an AD patient is shown in Figure 5.

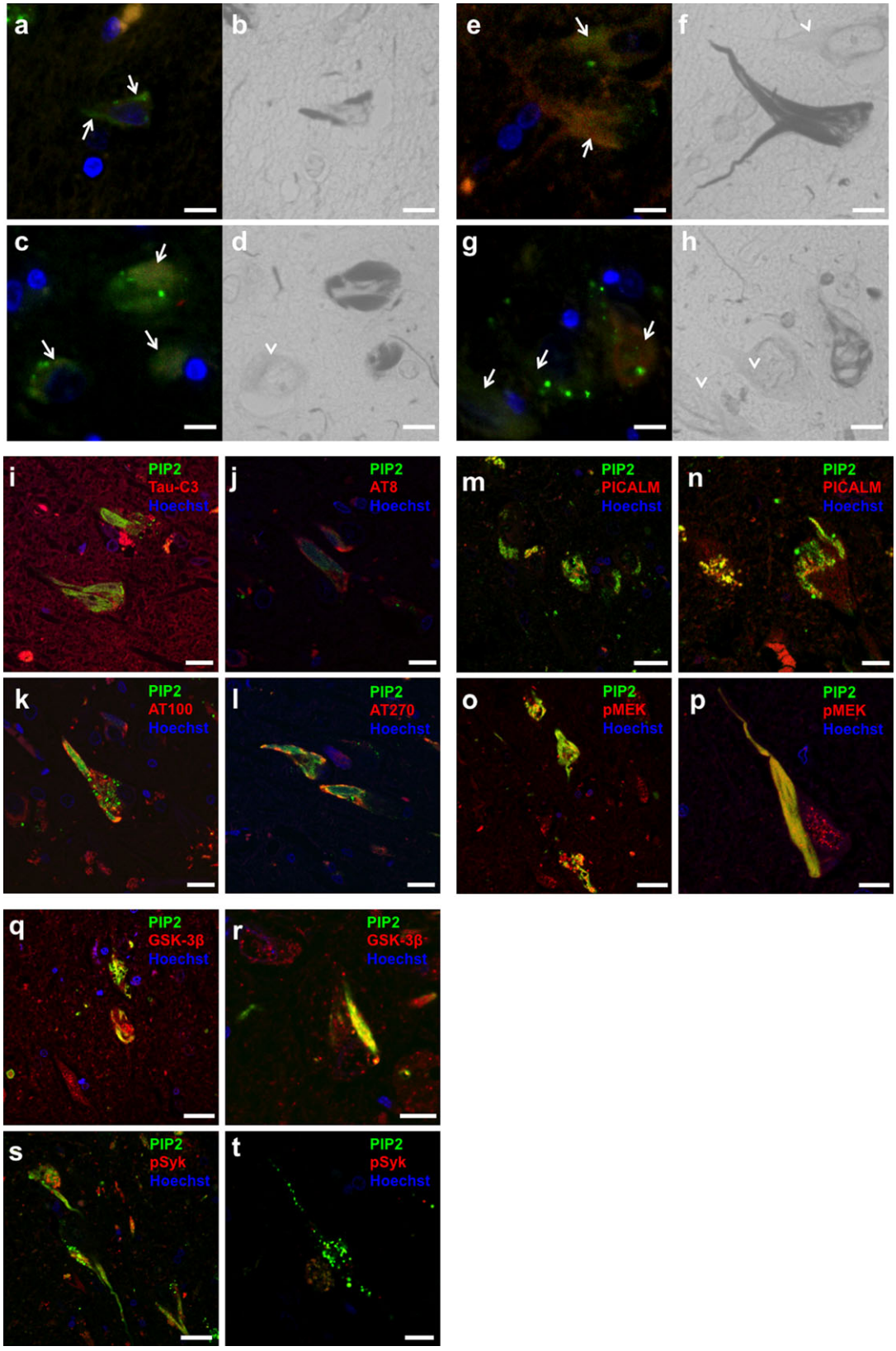

Several vesicular structures with a diameter of approximately 1 μm that contained central granules surrounded by a halo-like clear zone and an outer membrane, which structurally resembled GVD bodies, were present in a gap between PHFs. Some of these structures contained granules with high electron density, and others had intraluminal granule formations. Such clusters of vesicles were surrounded by PHFs.

Discussion

Previously, we showed that PtdIns(4,5)P2 is enriched in both GVD bodies and NFTs. We have also demonstrated that these structures are immunopositive for the raft marker flotillin-1, indicative of its association with lipid raft domains. In this study, we analysed PtdIns(4,5)P2-immunopositive material in detail, using super resolution and electron microscopy and found that the PtdIns(4,5)P2-immunopositivity that accumulates in pretangles corresponds to small vesicles with a mean diameter of approximately 1 μm. Double immunofluorescence staining for PtdIns(4,5)P2 and AT8 and electron microscopic images showed that the PtdIns(4,5)P2-immunopositive vesicles were surrounded by PHFs in a'islands in the sea' pattern (Figure 6). Gray *et al.* [28] observed that PHFs originate from the surface of membranous structures that often contain dense granules. In addition to flotillin-1, these PtdIns(4,5)P2-immunopositive raft-derived vesicles contain several tau kinases, suggesting that the vesicles have some role in the formation of PHFs. To our knowledge, such raft-derived tau-associated vesicles (hereafter referred to as RTVs) have not previously been described in detail.

We and others have reported the accumulation of flotillin-1-immunopositive vesicles in the pyramidal neurons of AD patients [5]. Flotillin-1 is integrated into lipid raft microdomains via palmitoylation and mediates endocytosis upon receptor stimulation. Several lines of evidence indicate that flotillin microdomains represent assembly sites for active signalling platforms [29,30]. Recently, apart from tau, several molecules, including several lipid raft-associated proteins such as annexin 2 [31], and tau kinases, such as GSK-3β [31], have been reported to accumulate in the pyramidal neurons of AD patients. PICALM is colocalized with phosphorylated tau not only in NFTs but also in GVD bodies [25]. The presence of PICALM is notable due to its ability to bind with PtdIns(4,5)P2 [32], suggesting it is associated with PtdIns(4,5)P2-immunopositive RTVs. Although the vesicular-staining pattern of PICALM resembles that of PtdIns(4,5)P2, PICALM has been reported to be localized on PHFs and not on vesicular structures. Pei and colleagues demonstrated the accumulation of CDK5 in the neurons of individuals in the early stages of AD [10]. We have previously shown that CDK5-immunopositive granules are present in hippocampal neurons and colocalize with AT8-immunopositive phosphorylated tau proteins. Syk, a newly identified tau kinase [26] that acts downstream of the TREM2 signalling cascade, is expressed in the hippocampal pyramidal neurons of patients with Nasu–Hakola disease and AD and is detected in GVD bodies [27]. Although little is known about the role of Syk in AD, it is noteworthy that TREM2 variants are a risk factor for AD. In this study, we revealed that Syk expressed in pyramidal neurons is localized to RTVs as well as to GVD bodies. Accordingly, the increase in the levels of multiple tau kinases in pyramidal neurons seems to coincide with the accumulation of RTVs. Recently, it was demonstrated that endosomal membranes can serve as a recruitment platform for sig-

Figure 3. Double immunofluorescence staining for phosphatidylinositol-4,5-bisphosphate [PtdIns(4,5)P2] (green) and charged multivesicular body protein 2B (CHMP2B) (red) (**a**), PtdIns(4,5)P2 (green) and AT8 (red) (**c**), PtdIns(4,5)P2 (green) and RD4 (red) (**e**), and PtdIns(4,5)P2 (green) and RD3 (red) (**g**) in neuronal cells in an Alzheimer's disease case. Thereafter, the same sections were subjected to Gallyas-Braak staining (**b**, **d**, **f**, **h**). PtdIns(4,5)P2-immunopositive fine granules that were immunonegative for CHMP2B and segregated from AT8 colocalized with RD4 but not with RD3 (arrows). Some of their regions were negative for Gallyas-Braak stain, indicating that they were pretangles (arrowheads). Double immunofluorescence staining for PtdIns(4,5)P2 (green) and Tau-C3 (red) (**i**), PtdIns(4,5)P2 (green) and AT8 (red) (**j**), PtdIns(4,5)P2 (green) and AT100 (red) (**k**), and PtdIns(4,5)P2 (green) and AT270 (red) (**l**). PtdIns(4,5)P2-immunopositive small granules were colocalized with Tau-C3 but not with AT8, AT100 or AT270, as shown in the spectrally unmixed images. Double immunofluorescence staining for PtdIns(4,5)P2 (green) and phosphatidylinositol-binding clathrin assembly protein (PICALM) (red) (**m**, **n**), PtdIns(4,5)P2 (green) and pMEK (red) (**o**, **p**), PtdIns(4,5)P2 (green) and glycogen synthase kinase (GSK)-3β (red) (**q**, **r**) and PtdIns(4,5)P2 (green) and phosphorylated spleen tyrosine kinase (pSyk) (red) (**s**, **t**). PtdIns(4,5)P2-immunopositive small granules were colocalized with PICALM, pMEK and several tau kinases, such as GSK-3β and pSyk. Scale bars: 10 μm (**a**–**l**, **n**, **p**, **r**, **t**), 20 μm (**m**, **o**, **q**, **s**).

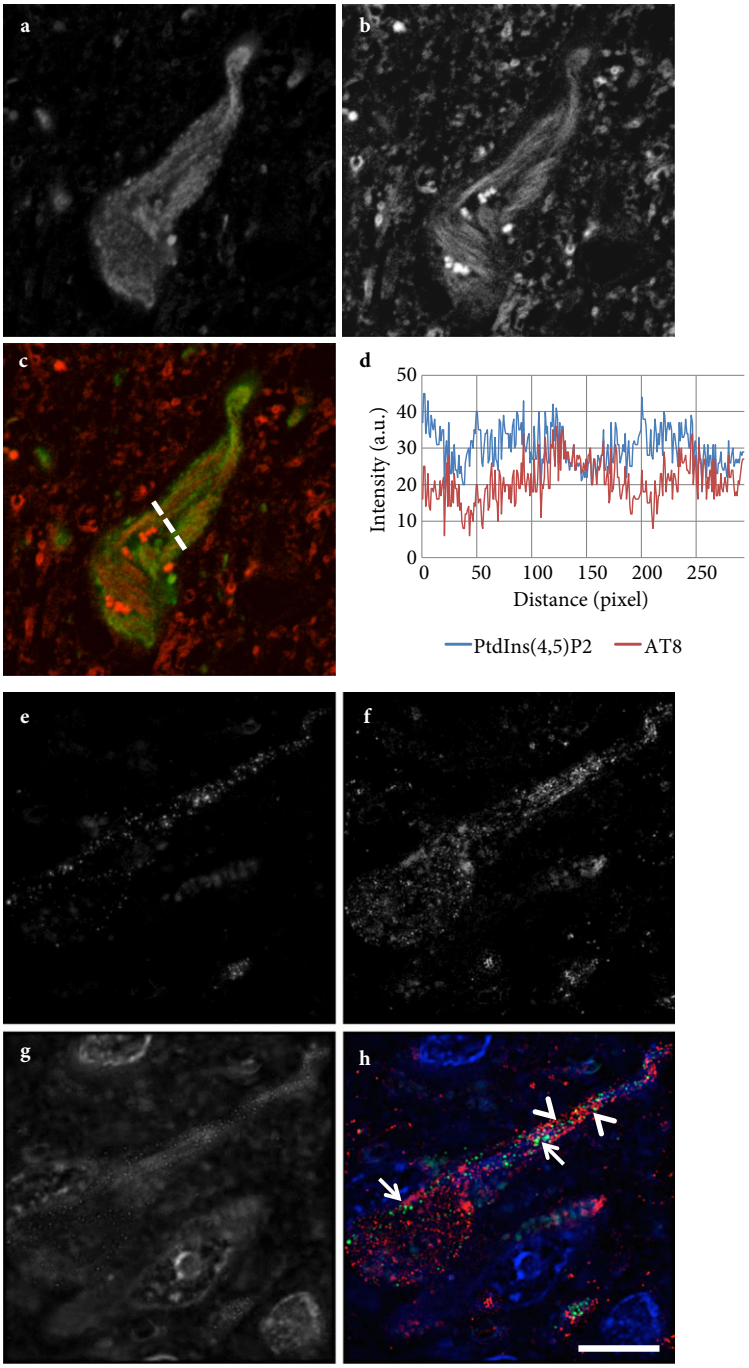

Figure 4. Colocalization analysis of phosphatidylinositol-4,5-bisphosphate [PtdIns(4,5)P2] with AT8 in a neuronal cell in an Alzheimer's disease (AD) case. Double immunofluorescence staining for PtdIns(4,5)P2 (**a**) and AT8 (**b**) and the pseudocoloured image for PtdIns(4,5)P2 (green) and AT8 (red) (**c**). The fluorescence intensity profile along the white dotted line is shown in (**d**). au, arbitrary unit. The inverse correlation between PtdIns(4,5)P2 and AT8 indicates that these molecules segregated from each other. Super-resolution microscopic image of PtdIns(4,5)P2- and AT8-immunopositive structures in a neuronal cell in an AD case, as revealed by double immunofluorescence staining (**e**–**h**); PtdIns(4,5)P2 (e), AT8 (**f**), Hoechst (**g**) and the superimposed image (**h**). A number of PtdIns(4,5)P2-immunopositive granules are sprinkled over the granular and filamentous materials that are immunopositive for AT8 (arrowheads). Some PtdIns(4,5)P2-immunopositive granules formed aggregates and were accompanied by a halo-like clear zone (arrows), suggesting that they were granulovacuolar degeneration bodies. Scale bars: 10 μm.

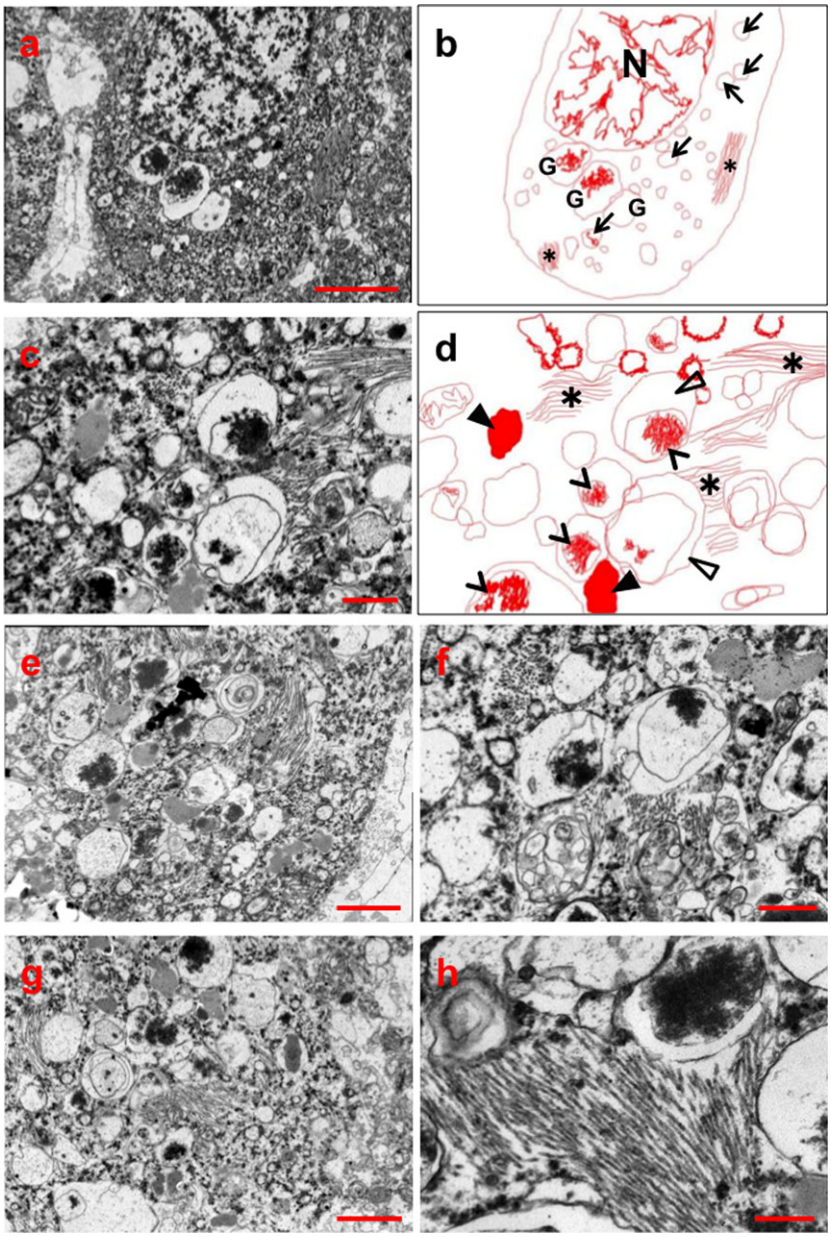

Figure 5. Electron microscopic images of phosphatidylinositol-4,5-bisphosphate-immunopositive vesicles in a neuronal cell in an Alzheimer's disease (AD) case. Panels **b** and **d** were produced by tracing the pictures in **a** and **c**. Several granulovacuolar degeneration bodies (G) and smaller vesicles with a diameter of 1 μm (arrows) were present in the cytoplasm around the nucleus (N) of a neuronal cell, and some of them contained granules with high electron density (arrowheads) that were distinct from lipofuscin (filled triangles) and/or had intraluminal granule formations (empty triangles) adjacent to paired helical filaments (*). Other neuronal cells from the same AD case also contained similar structures within the cytoplasm (**e**–**h**). Scale bars: 5 μm (**a**, **b**), 2 μm (**e**, **g**), 1 μm (**c**, **d**, **f**), 500 nm (h).

nalling complexes that are regulated by scaffold proteins. These endosomes are called 'signaling endosomes' and use flotillin-1 as a scaffold protein [33–35]. The presence of flotillin-1 and an array of tau kinases on RTVs suggests that RTVs act as signalling endosomes on which the tau protein is phosphorylated. The retention of endosomes as RTVs and the sustained activation of tau kinases may be attributable to the impaired lysosomal degradation of the endocytic compartment for some unspecified reason [36]. Furthermore, because recent work has shown that anionic lipid membranes can themselves induce tau aggregation, the surfaces of

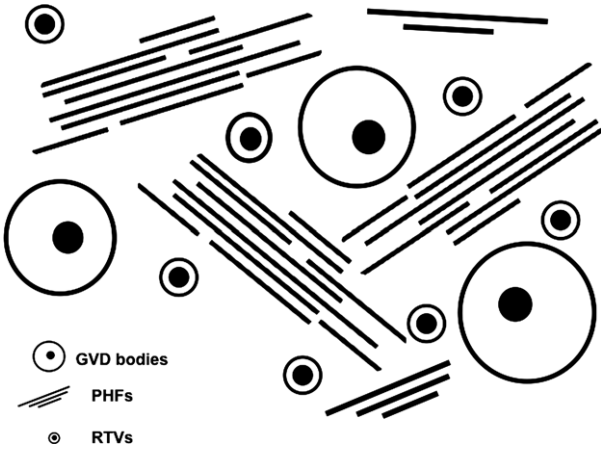

Figure 6. Proposed model for the spatial relationships between granulovacuolar degeneration (GVD) bodies, paired helical filaments (PHFs) and raft-derived tau-associated vesicles (RTVs). GVD bodies and RTVs are located adjacent to PHFs in an 'islands in the sea' pattern.

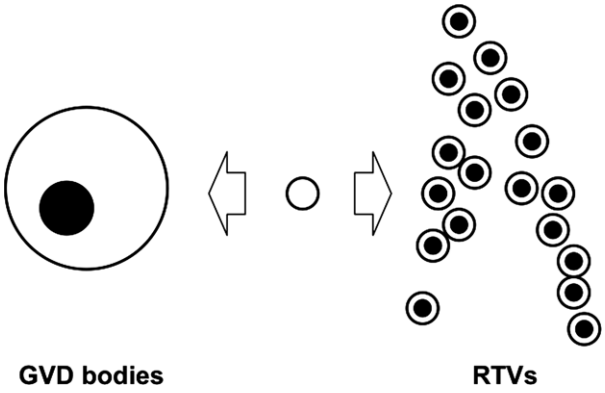

Figure 7. Proposed model for the relationship between granulovacuolar degeneration (GVD) bodies and raft-derived tau-associated vesicles (RTVs). RTVs fuse with each other and form GVD bodies. However, vesicles are clustered into RTVs, forming the outline of Neurofibrillary tangles.

RTVs, which contain negatively charged PtdIns(4,5)P2, may be a site at which PHFs accumulate and grow into NFTs [37,38]. This might explain why RTVs exist near PHFs.

Granulovacuolar degeneration bodies manifest as small inclusions that consist of 3- to 5-μm-diameter spherical vacuoles-containing argentophilic and electron-dense granules [1]. The presence of electron-dense granules is a shared feature of GVD bodies and RTVs. Okamoto *et al.* [12] reported the accumulation of small vesicles reminiscent of RTVs in close vicinity to GVD bodies by electron microscopic examination. Because of their morphological similarity, RTVs can be considered miniature GVD bodies, and it is likely that GVD bodies and RTVs have the same origin, as indicated by the similarity of their molecular profiles. Taking size into account, some vesicle fusion processes might lead to the formation of GVD bodies. Other than fusion, vesicles could cluster and pile up to create flame-shaped RTVs by an unknown mechanism (Figure 7). In addition to the difference in their size, however, RTVs differ from GVD bodies with respect to the presence of CHMP2B. CHMP2B is a subunit of the ESCRT III complex that mediates the formation of multivesicular bodies (MVBs) and/or amphisomes and is reported to be a marker of GVD bodies, but RTVs are negative for CHMP2B. The immunoreactivity of GVD bodies for CHMP2B suggests a failure of the MVBs to fuse with lysosomes in the endocytic pathway during the formation of GVD bodies; this could also account for the increased size of the vesicles. Therefore, the differences in the stages of vesicle trafficking may be reflected in the distinct properties of GVD bodies and RTVs (Table 2). The mode of accumulation of RTVs that precedes the maturation of NFTs would define the final

Table 2. Summary of the immunoreactive properties of GVD bodies and RTVs

	GVD body	*RTV*
Raft-related materials		
PtdIns(4,5)P2	(+)	(+)
PICALM	(+)	(+)
Flotillin-1	(+)	(+)
Annexin2	(+)	(+)
Tau kinases		
GSK3β	(+)	(+)
CK-1δ	(+)	(−)
CDK5	(+)	(+)
Syk	(+)	(+)
MEK	(+)	(+)
Endosome-related proteins		
CHMP2B	(+)	(−)
Modified tau proteins		
AT8	(−)	(−)
AT100	(−)	(−)
AT270	(−)	(−)
Tau-C3	(−)	(+)
RD4	(−)	(−)
RD3	(−)	(−)

(+) positive, (−) negative
GVD, granulovacuolar degeneration; RTV, raft-derived tau-associated vesicle; PtdIns(4,5)P2, phosphatidylinositol-4,5-bisphosphate; PICALM, phosphatidylinositol-binding clathrin assembly protein; GSK, glycogen synthase kinase; CK-1δ, casein kinase 1δ; CDK5, cyclin-dependent kinase 5; MEK, mitogen-activated protein kinase kinase; CHMP2B, charged multivesicular body protein 2B.

shape of the NFTs, and RTVs themselves would be another substructure of NFTs in addition to PHFs. The number of neurons with GVD bodies increases with the level of accumulation of phosphorylated tau [39], and GVD stage is correlated with the NFT stage [13]. Because the number of GVD bodies is followed by that of RTVs and because NFTs formation is preceded by RTV formation, RTVs may quantitatively connect GVD bodies and NFTs in various tauopathies.

In this study, we revealed that RTVs exist mainly in pretangles and NFTs at a relatively early stage. Pei *et al.* [28] reported that activated extracellular-signal-regulated protein kinase 1/2- and MEK 1/2-immunopositive granules are present in neuronal cells with NFTs and that these proteins are associated with the progression of neurofibrillary degeneration in AD. These granules resemble RTVs, in that they exist in early tangles and decrease in number during the maturation of tangles. Therefore, these proteins may be components of RTVs and associated with the generation of PHFs through tau phosphorylation.

Our study has several methodological limitations. We revealed the existence of RTVs in pretangles and showed their immunohistochemical profile but could not prove that RTVs form NFTs. To verify this possibility, an experimental system using animal models and cultured cell lines needs to be established.

In conclusion, we have demonstrated that clusters of raft-derived vesicles containing tau kinase form a substructure of pretangles distinct from PHFs. These vesicles are related to GVD bodies and are likely involved in the aggregation and modification of tau protein as well as, accordingly, the formation of PHFs. Further investigation of the mechanisms underlying RTV formation will shed light on the pathological process behind AD.

Acknowledgements

The authors thank Ms. Sasanishi, Ms. Furuno, Ms. Hironaka and Ms. Matsumoto for their excellent technical assistance and the Analysis Center of Life Science, Hiroshima University, Hiroshima, Japan, for the use of its facilities. This work was supported by grants from the Japanese Ministry of Education, Culture, Sports, Science, and Technology to M. Matsumoto and in part by a grant from Merck Sharp and Dohme (MSD) K. K., Tokyo, Japan and the Smoking Research Foundation, Tokyo, Japan to T. Takahashi.

Author contributions

Conceived and designed the experiments: TN, TT, MN and MM. Performed the experiments: TN, TT and MN. Analysed the data: TN, TT and MN. Contributed reagents/materials/analysis tools: TN, TT, YM, YI and MM. TN, TT, MN, NH, HM, YI and MM wrote the paper.

Conflict of interest

The authors declare that they have no competing interests. All authors read and approved the final manuscript.

References

1 Woodard JS. Clinicopathologic significance of granulovacuolar degeneration in Alzheimer's disease. *J Neuropathol Exp Neurol* 1962; **21**: 85–91.
2 Yamazaki Y, Takahashi T, Hiji M, Kurashige T, Izumi Y, Yamawaki T, Matsumoto M. Immunopositivity for ESCRT-III subunit CHMP2B in granulovacuolar degeneration of neurons in the Alzheimer's disease hippocampus. *Neurosci Lett* 2010; **21**: 86–90.
3 Nakamori M, Takahashi T, Yamazaki Y, Kurashige T, Yamawaki T, Matsumoto M. Cyclin-dependent kinase 5 immunoreactivity for granulovacuolar degeneration. *NeuroReport* 2012; **24**: 867–72.
4 Nishikawa T, Takahashi T, Nakamori M, Yamazaki Y, Kurashige T, Nagano Y, Nishida Y, Izumi Y, Matsumoto M. Phosphatidylinositol-4,5-bisphosphate is enriched in granulovacuolar degeneration bodies and neurofibrillary tangles. *Neuropathol Appl Neurobiol* 2014; **40**: 489–501.
5 Girardot N, Allinquant B, Langui D, Laquerriere A, Dubois B, Hauw JJ, Duyckaerts C. Accumulation of flotillin-1 in tangle-bearing neurones of Alzheimer's disease. *Neuropathol Appl Neurobiol* 2003; **29**: 451–61.
6 Yamaguchi H, Ishiguro K, Uchida T, Takashima A, Lemere CA, Imahori K. Preferential labeling of Alzheimer neurofibrillary tangles with antisera for tau protein kinase (TPK) I/glycogen synthase kinase-3 beta and cyclin-dependent kinase 5, a component of TPK II. *Acta Neuropathol* 1996; **92**: 232–41.
7 Ghoshal N, Smiley JF, DeMaggio AJ, Hoekstra MF, Cochran EJ, Binder LI, Kuret J. A new molecular link between the fibrillar and granulovacuolar lesions of Alzheimer's disease. *Am J Pathol* 1999; **155**: 1163–72.

8 Schwab C, DeMaggio AJ, Ghoshal N, Binder LI, Kuret J, McGeer PL. Casein kinase 1 delta is associated with pathological accumulation of tau in several neurodegenerative diseases. *Neurobiol Aging* 2000; **21**: 503–10.
9 Kannanayakal TJ, Tao H, Vandre DD, Kuret J. Casein kinase-1 isoforms differentially associate with neurofibrillary and granulovacuolar degeneration lesions. *Acta Neuropathol* 2006; **111**: 413–21.
10 Pei JJ, Grundke-Iqbal I, Iqbal K, Bogdanovic N, Winblad B, Cowburn RF. Accumulation of cyclin-dependent kinase 5 (cdk5) in neurons with early stages of Alzheimer's disease neurofibrillary degeneration. *Brain Res* 1998; **29**: 267–77.
11 Augustinack JC, Sanders JL, Tsai LH, Hyman BT. Colocalization and fluorescence resonance energy transfer between cdk5 and AT8 suggests a close association in pre-neurofibrillary tangles and neurofibrillary tangles. *J Neuropathol Exp Neurol* 2002; **61**: 557–64.
12 Okamoto K, Hirai S, Iizuka T, Yanagisawa T, Watanabe M. Reexamination of granulovacuolar degeneration. *Acta Neuropathol* 1991; **82**: 340–5.
13 Thal DR, Del Tredici K, Ludolph AC, Hoozemans JJ, Rozemuller AJ, Braak H, Knippschild U. Stages of granulovacuolar degeneration: their relation to Alzheimer's disease and chronic stress response. *Acta Neuropathol* 2011; **122**: 577–89.
14 Thal DR, Rub U, Orantes M, Braak H. Phases of A beta-deposition in the human brain and its relevance for the development of AD. *Neurology* 2002; **25**: 1791–800.
15 Braak H, Braak E. Neuropathological stageing of Alzheimer-related changes. *Acta Neuropathol* 1991; **82**: 239–59.
16 Mirra SS, Heyman A, McKeel D, Sumi SM, Crain BJ, Brownlee LM, Vogel FS, Hughes JP, van Belle G, Berg L. The Consortium to Establish a Registry for Alzheimer's Disease (CERAD). Part II. Standardization of the neuropathologic assessment of Alzheimer's disease. *Neurology* 1991; **41**: 479–86.
17 Hyman BT, Phelps CH, Beach TG, Bigio EH, Cairns NJ, Carrillo MC, Dickson DW, Duyckaerts C, Frosch MP, Masliah E, Mirra SS, Nelson PT, Schneider JA, Thal DR, Thies B, Trojanowski JQ, Vinters HV, Montine TJ. National Institute on Aging-Alzheimer's Association guidelines for the neuropathologic assessment of Alzheimer's disease. *Alzheimers Dement* 2012; **8**: 1–13.
18 Uchihara T, Nakamura A, Yamazaki M, Mori O, Ikeda K, Tsuchiya K. Different conformation of neuronal tau deposits distinguished by double immunofluorescence with AT8 and thiazin red combined with Gallyas method. *Acta Neuropathol* 2001; **102**: 462–6.
19 Matsudaira T, Uchida Y, Tanabe K, Kon S, Watanabe T, Taguchi T, Arai H. SMAP2 regulates retrograde transport from recycling endosomes to the Golgi. *PLoS ONE* 2013; **8**: e69145.
20 Lawo S, Hasegan M, Gupta GD, Pelletier L. Subdiffraction imaging of centrosomes reveals higher-order organizational features of pericentriolar material. *Nat Cell Biol* 2012; **14**: 1148–58.
21 Hara M, Hirokawa K, Kamei S, Uchihara T. Isoform transition from four-repeat to three-repeat tau underlies dendrosomatic and regional progression of neurofibrillary pathology. *Acta Neuropathol* 2013; **125**: 565–79.
22 Gamblin TC, Chen F, Zambrano A, Abraha A, Lagalwar S, Guillozet AL, Lu M, Fu Y, Garcia-Sierra F, LaPointe N, Miller R, Berry RW, Binder LI, Cryns VL. Caspase cleavage of tau: linking amyloid and neurofibrillary tangles in Alzheimer's disease. *Proc Natl Acad Sci USA* 2003; **19**: 10032–7.
23 Luna-Munoz J, Chavez-Macias L, Garcia-Sierra F, Mena R. Earliest stages of tau conformational changes are related to the appearance of a sequence of specific phospho-dependent tau epitopes in Alzheimer's disease. *J Alzheimers Dis* 2007; **12**: 365–75.
24 Hoozemans JJ, van Haastert ES, Nijholt DA, Rozemuller AJ, Eikelenboom P, Scheper W. The unfolded protein response is activated in pretangle neurons in Alzheimer's disease hippocampus. *Am J Pathol* 2009; **174**: 1241–51.
25 Ando K, Brion JP, Stygelbout V, Suain V, Authelet M, Dedecker R, Chanut A, Lacor P, Lavaur J, Sazdovitch V, Rogaeva E, Potier MC, Duyckaerts C. Clathrin adaptor CALM/PICALM is associated with neurofibrillary tangles and is cleaved in Alzheimer's brains. *Acta Neuropathol* 2013; **125**: 861–78.
26 Lebouvier T, Scales TM, Hanger DP, Geahlen RL, Lardeux B, Reynolds CH, Anderton BH, Derkinderen P. The microtubule-associated protein tau is phosphorylated by Syk. *Biochim Biophys Acta* 2008; **1783**: 188–92.
27 Satoh J, Tabunoki H, Ishida T, Yagishita S, Jinnai K, Futamura N, Kobayashi M, Toyoshima I, Yoshioka T, Enomoto K, Arai N, Saito Y, Arima K. Phosphorylated Syk expression is enhanced in Nasu-Hakola disease brains. *Neuropathology* 2012; **32**: 149–57.
28 Pei JJ, Braak H, An WL, Winblad B, Cowburn RF, Iqbal K, Grundke-Iqbal I. Up-regulation of mitogen-activated protein kinases ERK1/2 and MEK1/2 is associated with the progression of neurofibrillary degeneration in Alzheimer's disease. *Brain Res Mol Brain Res* 2002; **30**: 45–55.
29 Otto GP, Nichols BJ. The roles of flotillin microdomains–endocytosis and beyond. *J Cell Sci* 2011; **1**: 3933–40.
30 Miaczynska M, Pelkmans L, Zerial M. Not just a sink: endosomes in control of signal transduction. *Curr Opin Cell Biol* 2004; **16**: 400–6.
31 Leroy K, Boutajangout A, Authelet M, Woodgett JR, Anderton BH, Brion JP. The active form of glycogen

synthase kinase-3beta is associated with granulovacuolar degeneration in neurons in Alzheimer's disease. *Acta Neuropathol* 2002; **103**: 91–99.
32 Ford MG, Pearse BM, Higgins MK, Vallis Y, Owen DJ, Gibson A, Hopkins CR, Evans PR, McMahon HT. Simultaneous binding of PtdIns(4,5)P2 and clathrin by AP180 in the nucleation of clathrin lattices on membranes. *Science* 2001; **9**: 1051–5.
33 Grimes ML, Zhou J, Beattie EC, Yuen EC, Hall DE, Valletta JS, Topp KS, LaVail JH, Bunnett NW, Mobley WC. Endocytosis of activated TrkA: evidence that nerve growth factor induces formation of signaling endosomes. *J Neurosci* 1996; **15**: 7950–64.
34 Howe CL, Mobley WC. Signaling endosome hypothesis: a cellular mechanism for long distance communication. *J Neurobiol* 2004; **5**: 207–16.
35 Palfy M, Remenyi A, Korcsmaros T. Endosomal crosstalk: meeting points for signaling pathways. *Trends Cell Biol* 2012; **22**: 447–56.
36 Funk KE, Mrak RE, Kuret J. Granulovacuolar degeneration (GVD) bodies of Alzheimer's disease (AD) resemble late-stage autophagic organelles. *Neuropathol Appl Neurobiol* 2011; **37**: 295–306.
37 Jones EM, Dubey M, Camp PJ, Vernon BC, Biernat J, Mandelkow E, Majewski J, Chi EY. Interaction of tau protein with model lipid membranes induces tau structural compaction and membrane disruption. *Biochemistry* 2012; **27**: 2539–50.
38 Meister M, Tomasovic A, Banning A, Tikkanen R. Mitogen-activated protein (MAP) kinase scaffolding proteins: a recount. *Int J Mol Sci* 2013; **14**: 4854–84.
39 Yamazaki Y, Matsubara T, Takahashi T, Kurashige T, Dohi E, Hiji M, Nagano Y, Yamawaki T, Matsumoto M. Granulovacuolar degenerations appear in relation to hippocampal phosphorylated tau accumulation in various neurodegenerative disorders. *PLoS ONE* 2011; **6**: e26996.

Received 28 April 2015
Accepted after revision 7 October 2015
Published online Article Accepted on 26 October 2015